e-PLAS ANALYSIS OF SHORT PULSE LASER-MATTER INTERACTION EXPERIMENTS *

R. J. Mason[ξ,1], M. Wei and F. Beg[2], R. B. Stephens[3] and C. M. Snell[4]
[1]*Research Applications Corporation, Los Alamos, NM 87544,*
[2]*University of California, San Diego, CA 92093,* [3]*General Atomics, San Diego, CA 92121,*
[4]*Los Alamos National Laboratory, Los Alamos, NM 87545*

Abstract

The transport of relativistic electrons[1] generated in wire and foil targets by short-pulse lasers is examined with the new e-PLAS simulation code based on implicit-moment/hybrid[2] techniques. In a 50 μm diameter Cu wire (Z_{eff} = 15) as recently illuminated on the TITAN LLNL laser, for example, a $1.7x10^{20}$ W/cm^2 simulated laser beam delivering a flat 30 μm spot from the left (with 40 % absorption) generates the hot electron density profile depicted below at 940 fs. The peak hot density in the laser spot is ~$3x10^{21}$ electrons/cm^3. This density drops to $3x10^{19}$ electrons/cm^3 200 microns into the wire. A peak temperature of 2 keV is achieved through Joule heating of the background electrons in the wire "head" near the deposition surface; a significantly lower ~0.4 keV is achieved in the wire body. Here, 300 MG thermoelectric B-fields are also calculated. Parameter studies relate the hot electron stopping to the surface B-field, modest drag slowing, and the background cold electron resisitvity, which is bleached by background heating to low values at late times.

I. INTRODUCTION

Short pulse laser-matter experiments present a particular challenge to modeling. Large parts of the interacting plasma system are only mildly collisional, suggesting the use of particle-in-cell (PIC) techniques. Other closely coupled parts are fluidic and/or strongly collisional. The interacting region is often thousands of Debye lengths in scope, while traditional explicit PIC techniques require computational cells less than a Debye length in size.

To surmount these difficulties with some economy modelers have resorted to implicit coding, in which time advanced plasma currents are used to predict electric and magnetic (E- and B-*)* fields at the end of each computational cycle. In the Moment Method these advanced currents are obtained from a set of auxiliary fluid equations, used to advance accumulated densities and currents from an earlier cycle. Plasma particles and fluids are advanced in these predicted fields, yielding true currents that are subsequently used to correct the predicted fields for the next cycle.

We have applied this approach, as embodied in the e-PLAS code, to study the hot electrons generated in wire targets exposed to picosecond 1.06 μm laser pulses at 1.7 x 10^{20} W/cm^2 intensities. A typical target is sketched in Fig. 1

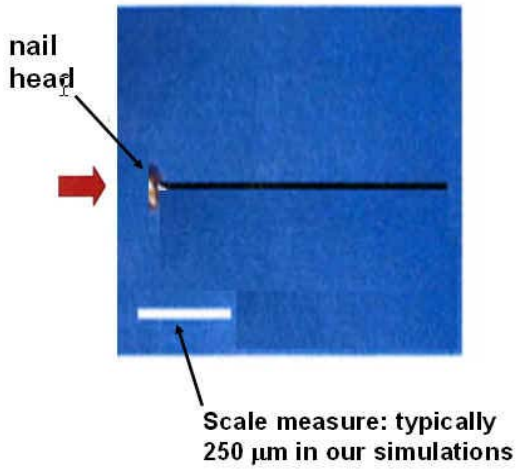

Figure 1. Nail target used in recent Titan laser experiments. The laser arrives from the left.

Hot electrons driven by the laser are typically generated at ponderomotive potential energies as predicted by Wilks[3], e.g. possessing here a relativisitic γ = 10.3. The wires are copper with an effective atomic number Z = 15. The hot electrons are stopped by drag against the background cold electrons, and by self-consistent *E*-fields arising from the resistance of the cold background returning to maintain charge neutrality. Relativistically corrected (using Jackson and Mosher's analysis) Spitzer resistivity and drag are employed. The resistivity is given a ceiling (for cold electron temperatures T_c < 100 eV) to replicate metallic limits. Heated colds are coupled to the ions at classical collisional rates. When $\nu_{c\text{-}i} \sim \nu_{h\text{-}c}$ cold heating is directly mirrored in the ions. However, we find that this is frequently not the case. Self-consistent B-fields can form thermoelectrically at the nail head surface

* Work supported in part by the USDOE through GA.
ξemail: rodmason01@msn.com

Report Documentation Page

Form Approved
OMB No. 0704-0188

1. REPORT DATE	2. REPORT TYPE	3. DATES COVERED
JUN 2007	**N/A**	**-**

4. TITLE AND SUBTITLE
E-Plas Analysis Of Short Pulse Lasermatter Interaction Experiments

5a. CONTRACT NUMBER
5b. GRANT NUMBER
5c. PROGRAM ELEMENT NUMBER

6. AUTHOR(S)

5d. PROJECT NUMBER
5e. TASK NUMBER
5f. WORK UNIT NUMBER

7. PERFORMING ORGANIZATION NAME(S) AND ADDRESS(ES)
Research Applications Corporation, Los Alamos, NM 87544,

8. PERFORMING ORGANIZATION REPORT NUMBER

9. SPONSORING/MONITORING AGENCY NAME(S) AND ADDRESS(ES)

10. SPONSOR/MONITOR'S ACRONYM(S)
11. SPONSOR/MONITOR'S REPORT NUMBER(S)

12. DISTRIBUTION/AVAILABILITY STATEMENT
Approved for public release, distribution unlimited

13. SUPPLEMENTARY NOTES
See also ADM002371. 2013 IEEE Pulsed Power Conference, Digest of Technical Papers 1976-2013, and Abstracts of the 2013 IEEE International Conference on Plasma Science. IEEE International Pulsed Power Conference (19th). Held in San Francisco, CA on 16-21 June 2013., The original document contains color images.

14. ABSTRACT
The transport of relativistic electrons1 generated in wire and foil targets by short-pulse lasers is examined with the new e-PLAS simulation code based on implicitmoment/ hybrid2 techniques. In a 50 ìm diameter Cu wire (Zeff = 15) as recently illuminated on the TITAN LLNL laser, for example, a 1.7x1020 W/cm2 simulated laser beam delivering a flat 30 ìm spot from the left (with 40 % absorption) generates the hot electron density profile depicted below at 940 fs. The peak hot density in the laser spot is ~3x1021 electrons/cm3. This density drops to 3x1019 electrons/cm3 200 microns into the wire. A peak temperature of 2 keV is achieved through Joule heating of the background electrons in the wire head near the deposition surface; a significantly lower ~0.4 keV is achieved in the wire body. Here, 300 MG thermoelectric B-fields are also calculated. Parameter studies relate the hot electron stopping to the surface Bfield, modest drag slowing, and the background cold electron resisitvity, which is bleached by background heating to low values at late times.

15. SUBJECT TERMS

16. SECURITY CLASSIFICATION OF:			17. LIMITATION OF ABSTRACT	18. NUMBER OF PAGES	19a. NAME OF RESPONSIBLE PERSON
a. REPORT	b. ABSTRACT	c. THIS PAGE			
unclassified	**unclassified**	**unclassified**	**SAR**	**4**	

and deflect hot electrons along it. For laser deposition we use a grid-following scheme, as in older hydro codes. The light follows the mesh to the neighborhood of the relativisitic critical density, and dumps a fraction of its energy there, in an emitted hot component. This can be either a hot fluid element or hot PIC particles. In the later case, the emission spectrum is either a relativistic Maxwellian, or a momentum shell, each at an energy specified by earlier classical PIC calculations. Similarly, the emission direction of particle electrons is pre-specified, as generally isotropic but possibly as a beam. The influence of a mean ponderomotive force is also included as a density-limited influence of the local gradient of the laser intensity.

II. NAIL/WIRE SIMULATIONS

e-PLAS has been applied to recent experiments at the Rutherford (RAL) Laboratory and at Livermore on its TITAN laser. In these experiments picosecond pulses at 1.06 μm and 0.1 to 1.7 x 10^{20} W/cm^2 were deposited onto the heads of copper nails (mean Z = 15). In simulation a flat pulse in planar polarization at normal incidence was deposited normally on nail heads, generally preceded by a 20 μm density ramp (from an assumed prepulse). The emitted hot electrons from this interaction were given an isotropic Maxwellian spectrum at ponderomotive energies, as predicted by Wilks[3], here, typically at a γ = 10.3.

In Fig. 2 we collect code prediction for hot electron transport and its consequences in a 50 μm diameter wire following 940 fs of illumination a 10 μm FWHM

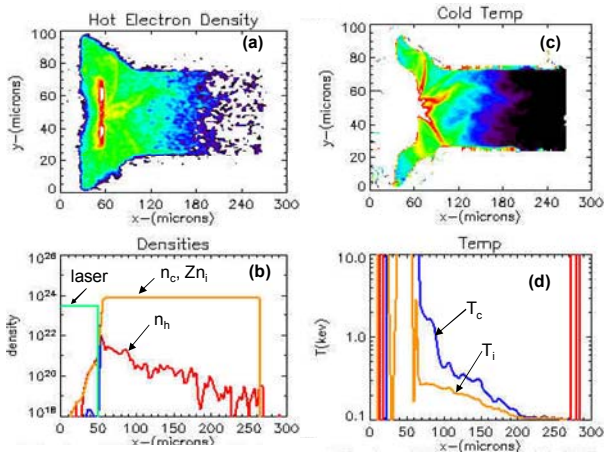

Figure 2. Conditions at 940 fs in the Cu wire. (a) hot electron density contours, (b) hot electron density, $n_h(x,y)$ on the centerline, (c) cold background temperatures $T_c(x,y)$, and (d) T_c and T_i (ion temperature) cuts at y = 50 μm.

Gaussian spot. The mesh is Cartesian. We see that hot electrons tend to remain trapped near the head. A bright "figure 8" shaped region marks the laser deposition region. Jets of hot electron run nearly vertically toward the head edges as well as axially down the wire. Hot electrons have reached a depth of about 150 μm. Thereafter, they show a spotty presence out to the back of the wire at 250 μm. The actual wire in the experiments was 1 mm long, so here we may see reflections off the back, absent in the real experiment.

Frame (b) shows that the peak hot electron density is nearly 10^{22} e$^-$/cm^3. A spike in density is coincident with the figure 8 hot spot, where the laser deposits. The hot density, n_h has decayed to 10^{20} e$^-$/cm^3 by x = 180 μm. In (c) and (d) we collect cold electron temperature, T_c data. In the head T_c reaches as much as 1.8 keV. Actually, right at the surface it rises to more than 10 keV, but we view such electrons as additional hot (or coronal) electrons. In some runs we have converted such coronal colds to hots, with no change for results inside the wire. In the main body of the wire beyond the head at 100 μm, the T_c remains below 400 eV, and the ions are slow to follow even in the head; they remain below 300 eV. Heated streamers of cold electrons are evident in frame (c), due to resistive heating of cold jets retracing (in reverse) the hot jet emission.

As in cone targets[1], resistive heating is the most dominant mechanism at early times in these wires. The E-field arising from this resistivity is captured in frame (d) of Fig. 3. It is evidently ~0.02 MeV/μm, so that over a distance of 100 μm, the hot electrons lose 2.0 MeV, clearly below their launch energy for γ = 10.3, i.e. 4.7 MeV.

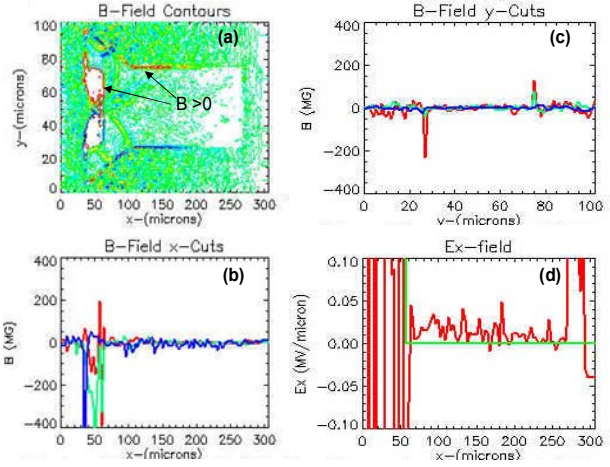

Figure 3. (a) Contours of the magnetic field in the nail head and wire body, (b) B-field in cuts 5 and 10 and 15 μm below the centerline, (c) vertical B-field cut at x = 120 μm, and (d) E-field along the centerline.

Magnetic fields in the head are positive above the centerline, characteristic of thermoelectric sourcing, i.e. electrons near the centerline are heading out toward the laser. The predicted B-ffields are intense near the head, exceeding 400 MG. The B > 0 value above the wire near 120 μm indicates a preponderance of hot electrons

transporting just outside the wire without a completely canceled cold return current.

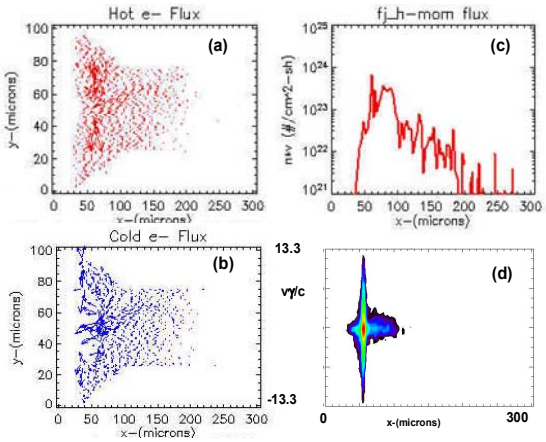

Figure 4. (a) flux of hot electron $n_h v_h$, (b) returning flux of cold background electrons $n_c v_c$, (c) $n_h v_h$ vs. depth x, and (d) hot electron phase space, f(u,x).

We collect flux data for the 50 μm wire experiment in Fig. 4. Clearly, the hot electron flux $n_h v_h$ is circulating in the head under the intense B-fields. Frame (b) shows how the cold electron flux responds, attempting to replace the hot electrons in their fountain toward the laser. Frame (c) shows that the hot flux decays exponentially over one order of magnitude from the head near x = 80 μm down to 180 μm. The final frame (d) shows that a major fraction of the electrons are captured near the head, consistent with the density spike near the laser source in Fig. 2 (b).

Recent experiments have focused on modifications in

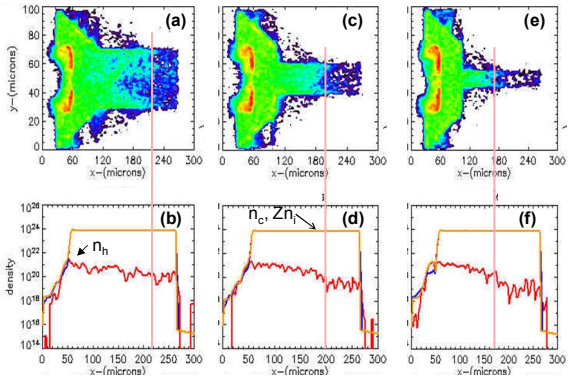

Figure 5. Density plots at 2 ps for wires with the diameter: (a,b) 40 μm, (c,d) 20 μm, and (e,f) 10 μm. The vertical line marks the maximum depth of high hot density.

the heating derived as the wire diameter was decreased for targets with a fixed head size. It appears that the wires become cooler with smaller diameters. In Fig. 5 we collect simulation results for diameters from 40 to 10 μm.

The figure shows decreased penetration of the hots as the wire diameter is decreased. In each case the peak n_h near the spot is of order 2 x 10^{21} e^-/cm^3. This hot density drops to 10^{20} e^-/cm^3 at 220, 200 and 170 μm, respectively, as the wire diameter is reduced from 40, through 20 to 10 μm. As earlier, the hot electrons tend to fill the head and accumulate brightly near the edges of the spot, where B-fields exceeding 300 MG are seen in all three cases.

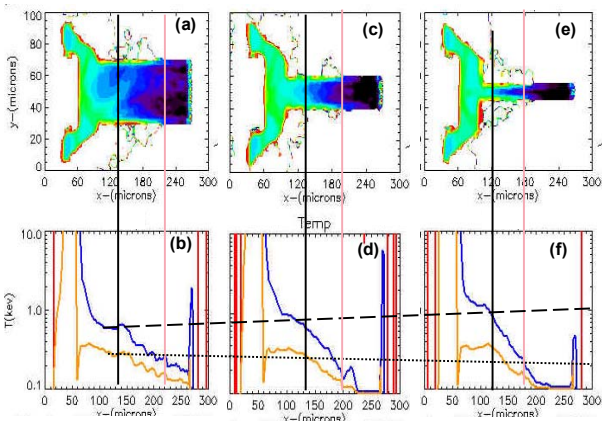

Figure 6. Cold electron temperature profiles $T_c(x,y)$ at 2 ps. Wires with diameters: (a) 40 μm, (c,d), 20 μm, and (e,f) 10 μm.

With Fig. 6 we capture the corresponding simulated cold electron temperature data. At 2 ps the colds in the wire at the same 220, 200, and 170 μm positions in our sequence of narrowed wires are 300, 250 and 200 eV, respectively. As the wires are parametrically narrowed, the cold temperature in the head rises from 600 to 900 eV at its base near 130 μm, testifying to more energy deposition there. The cold contours also show that cold surface heating is favored, presumably larger surface return currents allow for greater resistive heating there. In all cases, the ion temperatures remain well below the colds, even in the head; in (b) for example at 130 μm the ions reach only 300 eV, while the cold head electrons reach 600 eV.

We have done a few simulations with steep, 2 μm scale density ramps at the nail head, assuming colder hots (γ = 2.2) and greater absorption (80%), as might result light coupling directly to the densest points in the head[4]. Under such favorable but unlikely conditions, these simulations predict that the 20 μm wire could reach 2 keV at the x = 200 μm depth.

III. SUMMARY

Implicit plasma simulation can provide useful insight for short-pulse hot electron driven heating experiments. A significant fraction of the energy appears to remain in the nail head. The simulations show weak coupling to the ions. Higher absorption rates and lower hot energies from

possible steep density profiles can add to the cold heating, but such results exceed experimental findings.

IV. REFERENCES

[1] R. J. Mason, "Heating Mechanisms in Short-Pulse Laser-Driven Cone Targets," PRL **96**, 035001 (2006), and R. J. Mason, E. S. Dodd, and B. J. Albright, "Hot-electron surface retention in short-pulse laser-matter interactions," PRE **72,** 015401 (2005).

[2] R. J. Mason, and C. Cranfill, "Hybrid Two-dimensional Monte-Carlo Electron Transport in Self-consistent Electromagnetic Fields," IEEE Trans. Plasma Sci. **PS-14**, 45 (1986).

[3] S. C. Wilks, W. L. Kruer, M. Tabak, and A. B. Langdon, "Absorption of ultra-intense laser pulses," Phys. Rev. Lett. **69**, 1383 (1992).

[4] A. Kemp, Y. Sentoku, V. Sotnikov, "collisional Relaxation of Super Thermal Electrons Generated by Relativistic Laser Pulses in Dense Plasmas," Bull. Am. Phys. Soc. **51**, 348 (2006).